REPORT DOCUMENTATION PA[GE]

AD-A263 205

1. AGENCY USE ONLY (Leave blank)	2. REPORT DATE April 2, 1993	3. REPORT TYPE AND DATES COVERED Reprint

4. TITLE AND SUBTITLE Quasi-Static Model of Outer Zone Electrons	5. FUNDING NUMBERS PE 62101F PR 7601 TA 22 WU 03
6. AUTHOR(S) D.H. Brautigam, M.S. Gussenhoven, E.G. Mullen	
7. PERFORMING ORGANIZATION NAME(S) AND ADDRESS(ES) Phillips Lab/GPSP 29 Randolph Road Hanscom AFB, MA 01731-3010	8. PERFORMING ORGANIZATION REPORT NUMBER PL-TR-93-2076
9. SPONSORING/MONITORING AGENCY NAME(S) AND ADDRESS(ES)	10. SPONSORING/MONITORING AGENCY REPORT NUMBER

11. SUPPLEMENTARY NOTES

Reprinted from IEEE Transactions on Nuclear Science, Vol. 39, No. 6, Dec 1992

12a. DISTRIBUTION/AVAILABILITY STATEMENT Approved for public release; Distribution unlimited	12b. DISTRIBUTION CODE

13. ABSTRACT (Maximum 200 words)

With the Combined Release and Radiation Effects Satellite (CRRES) measurements, we have observed an extremely variable outer zone relativistic electron population from 25 July 1990 to 12 October 1991. Up to now, this population has been modeled by the static NASA solar minimum and maximum models. To address the inadequacies of using a static model to describe this highly dynamic environment, we develop a quasi-static model of the outer zone electrons based on the readily available geomagnetic activity index, Ap. It is shown that certain quantities used to parameterize the electron belt morphology are moderately correlated with the logarithm of the 15-day running average of Ap (Ap_{15}). We therefore separate and average, as a function of Ap_{15}, the 438 daily average radiation belt profiles (electron flux versus L) for each of 9 energy channels (1 - 8 MeV). The result is a set of average flux profiles which are keyed to geomagnetic activity. This quasi-static model provides a more accurate representation of the dynamic outer zone electron environment than could be expected from any static model.

14. SUBJECT TERMS Quasi-Static, Electrons, Flux, Magnetosphere	15. NUMBER OF PAGES 7
	16. PRICE CODE

17. SECURITY CLASSIFICATION OF REPORT	18. SECURITY CLASSIFICATION OF THIS PAGE	19. SECURITY CLASSIFICATION OF ABSTRACT	20. LIMITATION OF ABSTRACT
UNCLASSIFIED	UNCLASSIFIED	UNCLASSIFIED	SAR

QUASI-STATIC MODEL OF OUTER ZONE ELECTRONS

D.H. Brautigam, M.S. Gussenhoven, E.G. Mullen
Phillips Laboratory / GPSP, Hanscom AFB, MA 01731

Abstract

With the Combined Release and Radiation Effects Satellite (CRRES) measurements, we have observed an extremely variable outer zone relativistic electron population from 25 July 1990 to 12 October 1991. Up to now, this population has been modeled by the static NASA solar minimum and maximum models. To address the inadequacies of using a static model to describe this highly dynamic environment, we develop a quasi-static model of the outer zone electrons based on the readily available geomagnetic activity index, Ap. It is shown that certain quantities used to parameterize the electron belt morphology are moderately correlated with the logarithm of the 15-day running average of Ap (Ap_{15}). We therefore separate and average, as a function of Ap_{15}, the 438 daily average radiation belt profiles (electron flux versus L) for each of 9 energy channels (1 - 8 MeV). The result is a set of average flux profiles which are keyed to geomagnetic activity. This quasi-static model provides a more accurate representation of the dynamic outer zone electron environment than could be expected from any static model.

I. INTRODUCTION

The outer radiation zone of the magnetosphere is populated by trapped relativistic electrons lying between 2.4 and 8 Earth radii (R_E) that are only weakly confined to the magnetic equatorial plane [1]. It presents a serious radiation hazard to sensitive components in satellites and may limit the use of emerging technologies in space. Compared to energetic proton and electron populations in the inner radiation belt (within a radius of 1.8 R_E), the outer zone electrons exhibit large intensity fluctuations (several orders of magnitude in flux change) over short time periods (days) [2, 3]. The dynamical processes that drive these variations are still not identified, but many indicators of magnetospheric storm activity show some correlation, albeit weak, with outer zone intensifications [4, 5, 6]. Most of these studies have been conducted with data gathered on geosynchronous satellites flying at 6.6 R_E, a fixed altitude at the outer edges of the outer zone.

The high variability of the outer zone electrons presents a major modeling problem, both for the modeler and for the user. The NASA outer zone models (AE8MIN and AE8MAX for solar minimum and maximum, respectively) were prepared in the same way as the inner belt models, namely long-term averages applicable for missions 6 months or longer [7]. Thus, by their very nature they are inadequate for short missions. Moreover, recent comparisons of dose measured on orbit with predictions from the NASA models indicate that discrepancies of up to an order of magnitude exist even for long space flights, and can be in either direction depending on shielding thickness [8, 9].

A new opportunity to measure and model outer zone electrons is presented by the Combined Release and Radiation Effects Satellite (CRRES) which measured near-Earth particle populations over a wide energy range from 25 July 1990 to 12 October 1991. The CRRES orbit was a geosynchronous-transfer orbit with an 18° inclination. Its perigee was 350 km, and apogee, 33,500 km. With a period of about 10 hours, the satellite made at least four transits though the outer zone a day.

In this paper we report an effort to model the outer zone electron population in a fashion that gives a first order estimate of its dynamics. We model the outer belt over the electron energy range from 0.8 to 8 MeV using measurements from the High Energy Electron Fluxmeter (HEEF) onboard CRRES. We first establish that there is a moderate correlation between the electron fluxes and the 15-day running average of the global geomagnetic activity index, Ap, delayed by one day (referred to as Ap_{15}). The Ap index is made readily available by the NOAA-USAF Space Environment Services Center [10]. We then use Ap_{15} to construct eight average models of the electron flux variation with distance. The time history of the outer zone can then be roughly reconstructed for any time for which Ap exists using the eight models. The model fluxes and those of the NASA AE8MAX model are compared to the measured profiles to determine their relative accuracies and limitations in predicting the outer zone high energy electron population.

II. INSTRUMENTATION AND DATA HANDLING

The High Energy Electron Fluxmeter (HEEF) measures 0.8 to 8 MeV electrons in ten differential energy channels every 0.5 seconds. The instrument is a telescope, in design, having an acceptance half-angle of 10.5°. It is mounted perpendicular to the spin axis of the satellite, which in turn, points always in the solar direction. The satellite spin rate is 2 rpm. Both passive and active (triple coincidence) shielding are used to insure that high energy protons and low energy electrons do not contaminate the measurement. The instrument and its extensive pre-flight calibration are described in detail elsewhere [11]. The results presented here are based on a preliminary set of HEEF's calibration constants. A set of correction factors resulting from in-flight calibration analysis and further laboratory tests with HEEF's backup unit is forthcoming.

The time period represented in this study extends from 27 July 1990 to 11 October 1991, about 14 months. The database is generated from 30 second (1 spin) average HEEF fluxes

0018-9499/92$03.00 © 1992 IEEE

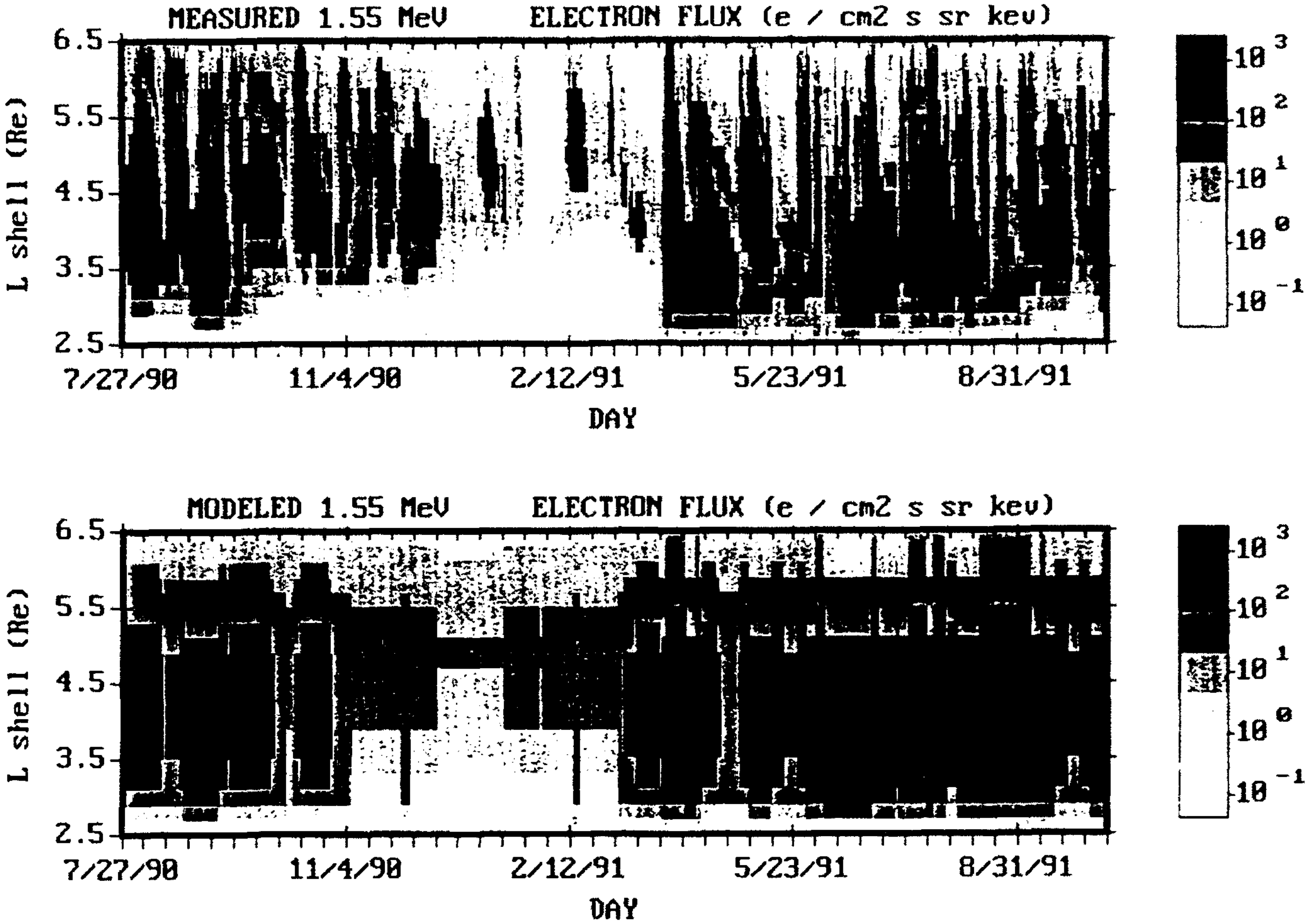

Figure 1. Measured (top panel) and modeled (bottom panel) daily averages of 1.55 MeV electron flux as a function of L (in R_E) and time (in days).

The average fluxes are accumulated in L-shell (L) bins of 0.2 R_E over the outer belt region from 2.4 to 6.6 R_E, independent of magnetic local time and magnetic field. The McIlwain L-parameter [12] is used instead of altitude because it identifies individual drift shells confining the electrons in their rotation around the Earth, eliminating the need to sort the data by local time or longitude. The Olson-Pfitzer tilt dependent magnetic field model [13] is used to determine L, and although the uncertainty in L increases for L > 4.5 during magnetically active periods, the model provides a reasonable basis for ordering the data. The data in each L bin is averaged to obtain a daily flux value for each altitude (L) and for each energy channel. These daily spin-averaged flux values are used to generate the models. We treat the spin averaged fluxes as unidirectional fluxes with units of e (cm^2 s sr keV)$^{-1}$. For this to be strictly valid, the electron population must be isotropic. This was determined to be approximately true after examining a database which is a superset (includes pitch angle information, and has a higher spatial resolution) of the one used in this study. We quantified the shape of each pitch angle distribution by defining a pitch angle index as follows. For a given pitch angle distribution, the electron flux was averaged over both 65-90° (j_{90}) and 40-65° (j_{65}) pitch angle intervals. A pitch angle index was then formed from the logarithm of the ratio j_{90} / j_{65} . Thus, a perfectly isotropic distribution would have an index of 0. An automated survey over the entire 1.5 MeV electron data set (restricted to L between 2.5 and 6.5) revealed that 81% of pitch angle distributions had an index between -.3 and +.3. In no cases did the index exceed an absolute value of 1.

III. Parameters for Describing and Ordering the Outer Zone Electron Flux Variations

The measured 1.55 MeV daily average electron fluxes over the CRRES mission lifetime are shown in the top panel of Figure 1 (the bottom panel will be discussed later). The flux values (encoded by gray scale) range from $<10^{-1}$ to $>10^3$ e (cm^2 s sr keV)$^{-1}$, and are plotted as a function of L (in R_E) on the vertical axis and time (in days) on the horizontal axis. The time interval between tick marks is 10 days. The wide variation in the radial position of the inner edge of high flux regions and the overall flux levels themselves is quite evident. For periods of more intense fluxes, the inner edge is located between 2.5-3 R_E and the fluxes peak above 10^3 e (cm^2 s sr keV)$^{-1}$. By contrast, days of less intense fluxes have an inner edge of maximum intensity around 4.5 R_E and a flux intensity peak below 10^2 e (cm^2 s sr keV)$^{-1}$. To illustrate these differences in more detail we show, in Figure 2, flux profiles as a function of L for 8 August 1990 and 8 January 1991, times of intense and weak outer zone electrons, respectively.

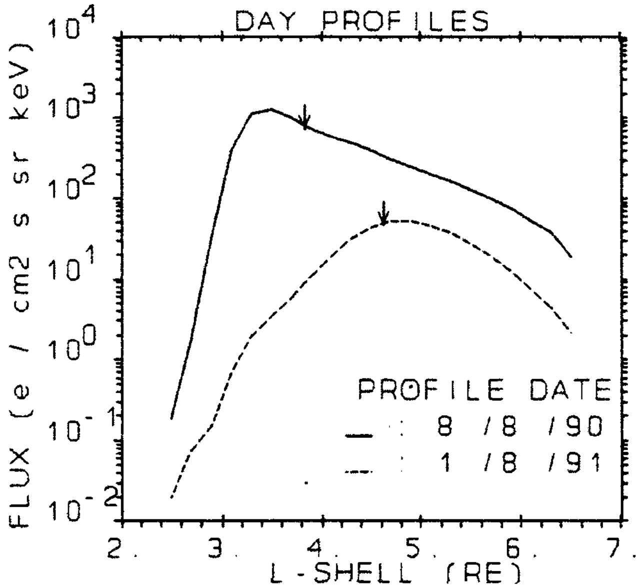

Figure 2. Electron flux intensity as a function of L-value, in Earth radii, for an intense outer zone (8 August 1990, solid line) and a weak outer zone (8 January 1991, dashed line). Arrows mark the centroid L of each profile (see text).

Not only do the flux peaks differ in intensity and position, but the form of the profile is extremely different in the two cases. The August profile rises steeply with increasing L and then falls off relatively slowly. The January profile both rises and falls off slowly, with similar slope magnitudes. To model the outer zone electrons we need to find an ordering parameter for these different profiles of electron flux intensity as a function of L. To do this we first characterize the profiles with two parameters likened, for a mass distribution, to the total mass and the center of mass.

For an individual flux profile, such as either of those shown in Figure 2, for a given energy channel, we define two parameters P_1, indicating flux intensity in the outer zone, and P_2, indicating the center of the flux distribution. We call P_1, the "profile flux" parameter. It is the integral of the flux over L:

$$P_1(E) = \sum_{i=1}^{21} j_i(E) * \Delta L_i$$

We call P_2, the "centroid L" parameter, defined in analogy to the center of mass as:

$$P_2(E) = \frac{\sum_{i=1}^{21} L_i * j_i(E) * \Delta L_i}{\sum_{i=1}^{21} j_i(E) * \Delta L_i}$$

In these equations:

L_i = L-shell bin midpoint in R_E (2.5 to 6.5 R_E);
delta L = L bin width (0.2 R_E);
i = L bin number (1 to 21); and
$j_i(E)$ = flux for a given energy channel (E) and L bin (i).

In Figure 2, arrows mark the centroid L for the two profiles at 3.8 and 4.6 R_E for the intense and weak profiles, respectively. The corresponding profile fluxes, P_1, are 1.4×10^3 and 7.3×10^1 having units of flux times R_E.

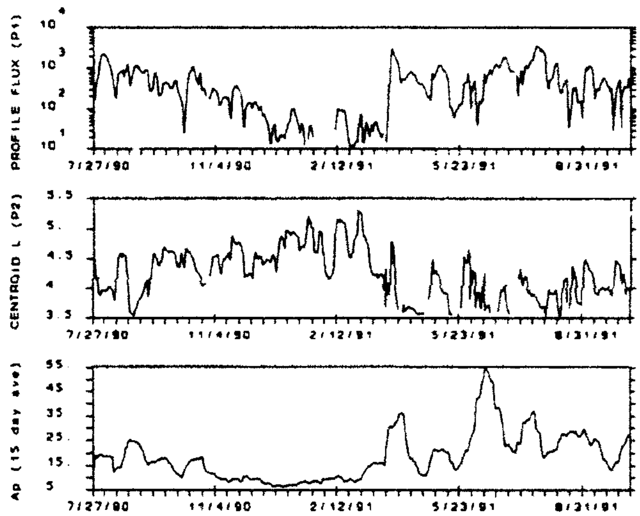

Figure 3. Profile flux (P_1; top panel) and centroid L (P_2; middle panel), as defined in the text, plotted versus time (in days). Both parameters were derived from daily 1.55 MeV fluxes. Fifteen day running average of Ap (Ap_{15}) versus time (in days) is plotted in bottom panel.

The two parameters defined above are calculated for electron flux profiles for each day of the CRRES mission and for each HEEF energy channel. Figure 3 shows these two parameters for 1.55 MeV electrons (P_1, top panel; P_2, middle panel) plotted versus day. The bottom panel is a 15 day running average of the Ap magnetic activity index (referred to as Ap_{15} for the remainder of this paper). Ap is a readily available index of magnetic activity, constructed from ground-based magnetic stations having a broad distribution in latitude and longitude [10]. Ap varies linearly with the magnitude of the magnetic disturbance. Figure 3 shows that magnetic activity was most quiet ($Ap_{15} \leq \sim 10$ nT) from November 1990 through February 1991. In this quiet period P_1 (profile flux) has relatively low values and P_2 (centroid L) has relatively high values. In general, as magnetic activity diminishes, P_1

(profile flux) decreases and P_2 (centroid L) increases. During periods of high magnetic activity the reverse is true, as can be seen in the periods before December 1990 and after March 1991. These trends are quantified in Figure 4 where P_1 (top panel) and P_2 (bottom panel) are plotted versus $\log(Ap_{15})$ with an imposed 1 day lag time. A lag time of 1 day was chosen because it was found to minimize the error between the measured and modeled fluxes to be discussed in the next section of this paper. A linear regression of the 437 data point yields a correlation coefficient of ~.65 for both the direct relation between P_1 and $\log(Ap_{15})$ and the inverse relation between P_2 and $\log(Ap_{15})$. The eight large dots on each plot refer to modeled parameters and will be addressed later. Given the moderate correlations between the flux profile parameters and $\log(Ap_{15})$, we use Ap_{15} to separate and bin the electron data to produce our flux models.

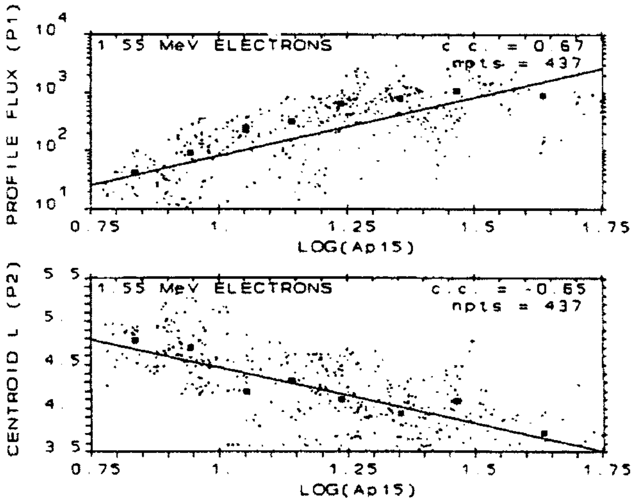

Figure 4. Profile flux (P_1; top panel) and centroid L (P_2; middle panel) plotted versus $\log(Ap_{15})$. A linear regression was performed on the 437 data points, with the best-fit line plotted and the correlation coefficient given in upper right corner of panel. Eight large dots are the profile parameters derived from the eight model profiles.

IV. OUTER ZONE ELECTRON MODELS

Because of the highly dynamic nature of the outer belt electrons, a single model to reproduce all conditions was deemed impractical. After much trial and error, we concluded that 8 models divided over the CRRES Ap_{15} range between 5 and 55 nT would give a good representation of most conditions measured on CRRES. All daily flux profiles corresponding to the days assigned to one of the 8 Ap_{15} intervals (assuming a 1 day lag time) were averaged together to determine the model profile for that activity level. For example, model profile #1 is the average of the individual flux profiles for the 31 days in which the value of Ap_{15} on the day preceding the daily flux profile was between 5 and 7.5 nT. A summary of the model inputs is given in Table I. Included in the table is the range and the corresponding average of Ap_{15}, the number of daily profiles used to compute the average, and the percent of the total days (438) used for the profile.

Table I - Ap_{15} Model Statistics

Model #	Ap_{15} (nT) Range	Ave Ap_{15} (nT)	Days per Model	% of Total
1	5.0-7.5	6.8	31	7.1
2	7.5-10.0	8.7	83	18.9
3	10.0-12.5	11.2	35	8.0
4	12.5-15.0	13.7	35	8.0
5	15.0-20.0	17.1	98	22.4
6	20.0-25.0	22.4	71	16.2
7	25.0-35.0	28.9	56	12.8
8	35.0-55.0	42.5	29	6.6

The resulting model profiles for four of the energy channels are shown in Figure 5 with electron flux plotted against L shell. For the sake of clarity, only every other model profile is displayed. Model profiles #1 and #2 (#1 is the bottom curve displayed in each plot) which were averaged from the extended quiet interval from November 1990 - February 1991, are significantly different in shape and magnitude from the remaining higher activity profiles. The higher activity profiles are themselves very similar in both shape and magnitude. To show how well the models can reproduce the original data, the P_1 and P_2 model parameters from the 1.55 MeV channel were calculated and plotted as solid circles on their respective plots of Figure 4. As expected, the model parameters P_1 and P_2 vary with $\log(Ap_{15})$ in the same way as do the daily profile parameters. This relationship holds true for all energy channels.

The model flux profiles ordered by geomagnetic activity shown in Figure 5 are also compared with the single flux profile for each of two static models briefly described next. To compare the new Ap dependent models with existing static models and data sets, the NASA solar maximum electron radiation belt model (AE8MAX) was used to construct a flux versus L profile for each energy channel of Figure 5. AE8MAX is a matrix of omnidirectional integral fluxes stored as a function of threshold energy, B/B_0, and L parameter [7]. B/B_0 is the ratio of the magnitude of the magnetic field at the point in question to that on the magnetic equator following the same field line, and is a measure of magnetic latitude. It, therefore, requires some preprocessing for a direct comparison with CRRES flux data. To use AE8MAX to predict the electron fluxes CRRES should see, CRRES orbits were traced through this matrix, and the omnidirectional integral fluxes converted to unidirectional differential fluxes for each of the CRRES electron energy channels. The comparison is shown in Figure 5 as the solid curve. In all energy channels the NASA model gives values higher than the CRRES models above an L of 5 R_E. For energies above about 2 MeV the NASA model gives higher values at all L values above ~3.4 R_E.

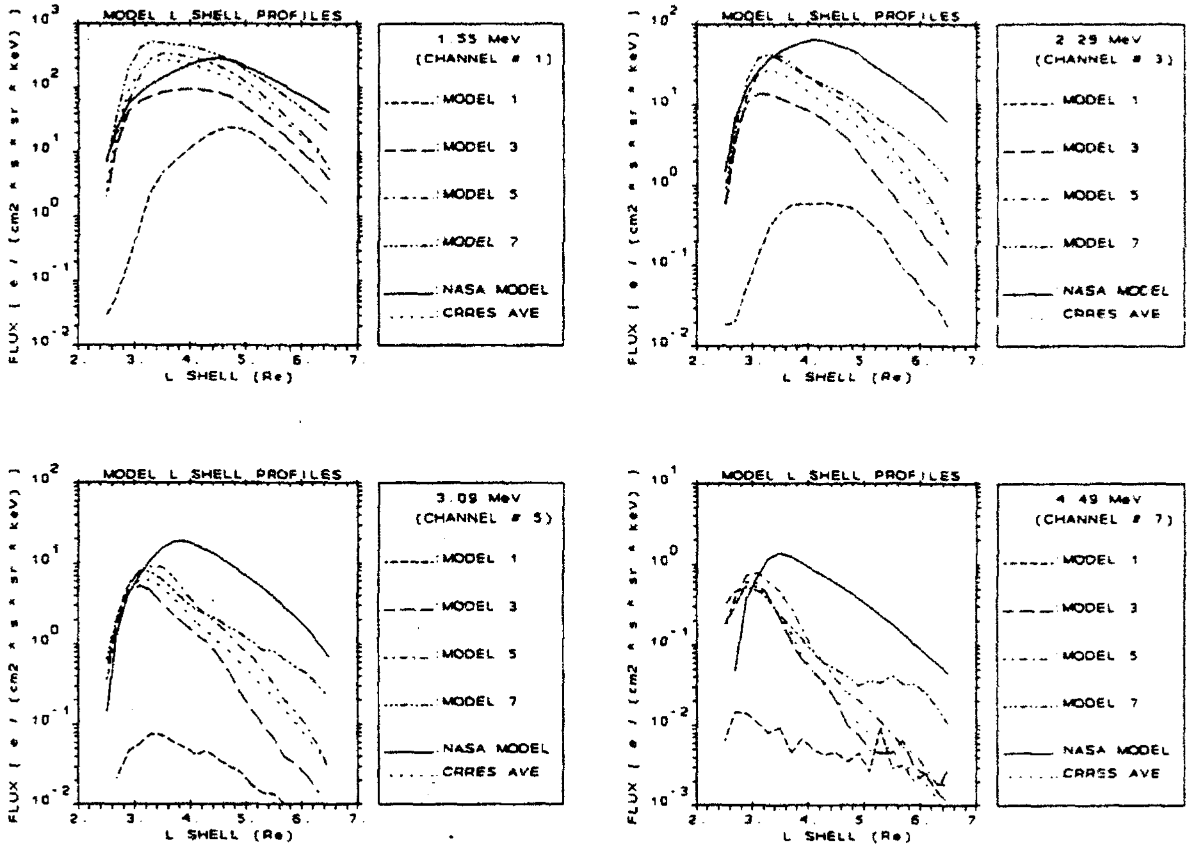

Figure 5. Eight Ap_{15} model profiles for 4 different energy channels (as specified in key). Also included are the NASA AE8MAX model (heavy solid line) and the CRRES-static model (dotted lines) profiles.

To show that the NASA model electron fluxes are indeed higher than all the CRRES data, and to illustrate the modeling benefit of quasi-static models relative to fully static models, we also created a single static model from the CRRES data. The CRRES-static model is simply an ordering of the full set of HEEF data by L shell (0.2 R_E bins) to yield one average flux profile for each energy channel. The electron flux profiles for the CRRES-static model are also included in Figure 5 and are drawn with dotted lines. The CRRES static model fluxes are, not surprisingly, similar to the quasi-static model fluxes for active magnetic conditions, since in linear averages of quantities varying by orders of magnitude, the high values will dominate. The profile intensity and shape of the average CRRES model fluxes are, however, still very different from and well below the NASA model levels.

V. Discussion And Conclusions

Since daily Ap magnetic indices are disseminated weekly [10], the quasi-static model presented here provides a method for calculating the short term average fluxes of the outer zone electron belts. To see how well this would have worked for CRRES while in flight, we used the daily values of Ap_{15} from Figure 3 to identify which model electron profile to use for each day of the CRRES mission. The survey plot derived from the models is plotted in the bottom panel of Figure 1 for direct visual comparison with the measured values. The agreement, although not perfect, is far better than any static model could give. The models maintain the overall gross features of the measured data such as the quiet interval during the middle of the mission and the various intensifications seen after March 1991.

Figure 6 quantifies the differences seen between the measured and modeled flux profiles. A "difference ratio" is computed for each L bin for each day of the mission. The ratio is defined as the absolute value of (measured flux - modeled flux) / measured flux. The three curves in Figure 6 are the fraction of days (y-axis) that the "difference ratio" calculated from the quasi-static Ap_{15} model, the NASA AE8MAX model and the CRRES-static model, is less than unity for each L (x-axis). In general terms, the plots represent the fraction of time the models give numbers within a factor of 2 of the measured values. Overall, the Ap_{15} quasi-static model gives the best agreement and the NASA AE8MAX the worst. The Ap_{15} models are within a factor of 2 of the measured values fairly consistently (50% of the time) over all L's from 2.5 to 6.5 R_E. The NASA model, on the other hand, shows serious problems for all but the lowest L-values.

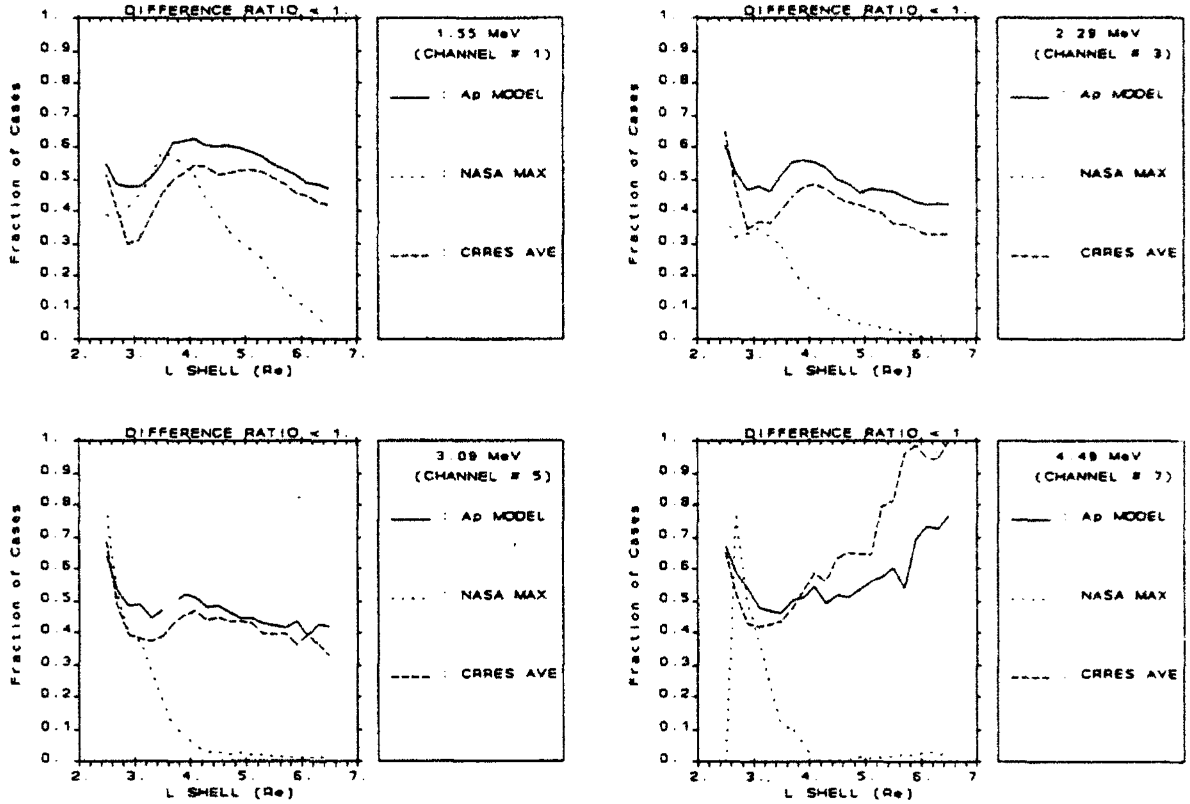

Figure 6. Line histogram for the case where the 'difference ratio' between the fluxes of the various models and the measured data is less than 1 for each L bin. The 'difference ratio' is defined as the absolute value of (measured flux-modeled flux)/measured flux.

Upon examination of individual spectral comparisons (not shown), it is seen that the NASA spectra are much harder than the CRRES spectra, with the result that NASA predicts much higher fluxes at higher energies up to 5 MeV which is consistent with the higher NASA predicted electron doses [8, 9].

In conclusion, the NASA models are the most widely used models for predicting electron radiation to near-Earth space systems. We have shown that the AE8MAX model has severe deficiencies when compared to recent CRRES measurements, particularly at energies > 2 MeV and for distances beyond 3.5 R_E. Trying to model a highly dynamic particle population with a single static model will never produce reasonable results under all conditions. As a minimum, two models, representing quiet and active magnetospheric conditions, are needed. The approach presented here, driven by the magnetic activity index Ap, provides a promising methodology for developing a fully functional quasi-static outer zone electron model. By supplementing the current CRRES database with future data sets to improve model statistics, this quasi-static model could become the standard for predicting electron fluxes (dose) for future space missions.

VI. References

[1] Spjeldvik, W.N., and R.L. Rothwell, "The Radiation Belts," Chapter 5 in Handbook of Geophysics and the Space Environment, edited by Adolph S. Jursa, Air Force Geophysics Laboratory, Hanscom AFB, MA, ADA167000, 1985.

[2] Vampola, A.L., J.B. Blake, and G.A. Paulikas, "A new study of the magnetospheric electron environment," J. Spacecraft and Rockets, 14, 690, 1977.

[3] Baker, D.N., J.B. Blake, R.W. Klebesadel, and P.R. Higbie, "Highly relativistic electrons in the Earth's outer magnetosphere: 1. Lifetimes and temporal history 1979-1984," J. Geophys. Res., 91, 44265, 1985.

[4] Paulikas, G.A., and J.B. Blake, "Modulation of trapped energetic electrons at 6.6 R_E by the direction of the interplanetary magnetic field," Geophys. Res. Lett., 3, 277, 1976.

[5] Paulikas, G.A., and J.B. Blake, "Effects of the solar wind on magnetospheric dynamics: Energetic electrons at the synchronous orbit," in Quantitative Modeling of Magnetospheric Processes, ed., W.P. Olson, Am. Geophys. Union, Washington, D.C., 180, 1979.

[6] Baker, D.N., P.R. Higbie, R.D. Belian, and E.W. Hones, Jr., "Do Jovian electron influence the terrestrial outer radiation zone?" Geophys. Res. Lett., 6, 531, 1979.

[7] Vette, J.I., The AE-8 Trapped Electron Model Environment, NSSDC 91-24, NASA GSFC, Greenbelt, MD, 1991.

[8] Gussenhoven, M.S., E.G. Mullen, R.C. Filz, D.H. Brautigam, and F.A. Hanser, "New low-altitude dose measurements," IEEE

Trans. Nucl. Sci., NS-34, 676, 1987.

[9] Gussenhoven, M.S., E.G. Mullen, D.H. Brautigam, E. Holeman, and C. Jordan, "Preliminary comparison of dose measurements on CRRES to NASA model predictions", IEEE, Trans. Nucl. Sci., NS-38, 1655, 1991.

[10] NOAA-USAF Space Environment Services Center, Preliminary Report and Forecast of Solar Geophysical Data, U.S. Dept. Commerce, NOAA, Boulder, CO, SESC PRF 776-841, 1990-1991.

[11] Dichter, B.K., and F.A. Hanser, Development and Use of Data Analysis Procedures for the CRRES Payloads AFGL-701-2/Dosimeter and AFGL-701-4/Fluxmeter and Application of the Data Analysis Results to Improve the Static and Dynamic Models of the Earth's Radiation Belts, Geophysics Laboratory Technical Report GL-TR-89-0284, Hanscom Air Force Base, MA, 1989.

[12] McIlwain, C.E., "Coordinates for mapping the distribution of magnetically trapped particles," J. Geophys. Res., 66, 3681, 1961.

[13] Olson, W.P., and Pfitzer, K. A., Magnetospheric Magnetic Field Modeling, Annual Scientific Report, AFOSR Contract No. F44620-75-C-0033, McDonnell Douglas Astronautics Company, Huntington Beach, CA, 1977.